Mm-Wave Outdoor-to-Indoor Channel Measurement In An Open Square Smallcell Scenario

Minseok Kim1, Tatsuki Iwata1, Kento Umeki1, Karma Wangchuk2, Jun-ichi Takada2, and Shigenobu Sasaki1,
1Graduate School of Science and Technology, Niigata University, Niigata, Japan
2Graduate School of Science and Engineering, Tokyo Institute of Technology, Tokyo, Japan

***Abstract* - This paper presented an outdoor-to-indoor (O2I) channel measurement result at 58.5 GHz assuming an outdoor hotspot access scenario in 5G mobile systems and WLANs. Comparing the measurement results with ray-tracing (RT) simulation, dominant propagation mechanisms were identified. From the analysis, the propagation mechanism of eight multi-path clusters were identified.**

***Index Terms* — channel sounding, millimeter wave, directional channel, polarization, indoor-to-outdoor channel.**

1. Introduction

Utilization of new radio spectrum at high frequency bands to accommodate the exploded traffic in 2020 and beyond is a very hot latest issue [1]. Since the frequency range from 24.25 GHz up to 86 GHz for future fifth generation (5G) mobile communications (called IMT-2020) has been identified in the world radio conference (WRC15) in 2015, the research and standardization activities are now being much accelerated. In this regard, radio propagation channel properties at high frequency bands should be carefully investigated. However, there are few reports on the propagation properties in outdoor-to-indoor (O2I) environments and the dominant propagation mechanisms have not been thoroughly investigated by multidimensional channel sounding measurements.

Among the various deployment scenarios in 5G and WLANs [2], [3], the urban micro-cellular (UMi) open square O2I is considered here. The user equipment (UE) is located in an indoor environment and the base station (BS) is located in an outdoor environments, for example, at a lamppost in an open square, neighboring building wall and so forth. This paper will present the channel measurement results in O2I scenario in Niigata university campus at an mm-wave band of 58.5 GHz. In this measurement, using the developed custom channel sounder which is configured in 2×2 MIMO (multiple-input-multiple-input) to measure full polarimetric channel responses simultaneously [4], [5], double-directional wideband channel transfer functions were measured by rotating high gain horn antennas. The dominant propagation mechanism will be discussed by comparison between the measurement and ray tracing (RT) simulation. The polarization properties of the observed dominant multi-path components will also be presented by using their polarimetric path gain.

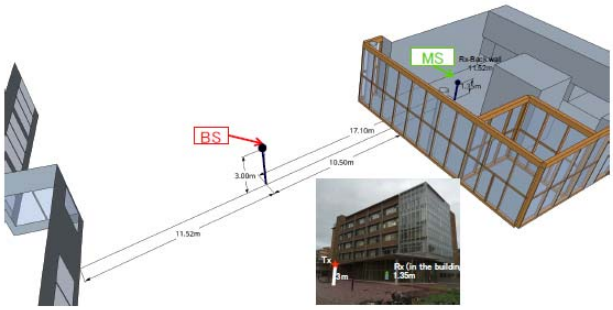

Fig. 1. Measurement campaign at the open area outdoor environment.

2. Measurement Campaign

The measurement campaign was conducted in an outdoor open square as shown in Fig. 1 [6] where Tx as a base station (BS) was located in an outdoor open area and the channel transfer functions were measured at the Rx in the first floor of the building where the building wall between the Tx and the Rx was entirely made in glass with metal frames. The antenna heights were 3 m for Tx (BS) and 1.35 m for Rx (UE), respectively. The measurement site was surrounded by some large buildings which were located 20~ 30 m far away from the Tx. The distances from the Tx to the building glass wall, and from the building glass wall to the Rx were approximately 10.50 and 6.60 m, respectively.

In the measurement, the developed custom channel sounder was used [5]. Using 2×2 MIMO configuration full polarimetric wideband channel transfer functions were simultaneously measured. The transmit power of approximately 10 dBm. We excluded the influence of the measurement system from the measured channel responses by full MIMO back-to-back calibration. The measurement dynamic range is limited to approximately 40 dB. For acquisition of full polarimetric double-directional channel transfer functions, two orthogonally polarized (ϕ and ϑ) high gain horn antennas were used at both sides of Tx and Rx, where those antennas were not co-located but direct toward the opposite side (180 degrees) on the same plane. The BS and MS antennas were rotated from 0 to 360 degrees in azimuth, and from −30 to 30 degrees in elevation. Because the half power beam-width (HPBW) are 30 degrees (gain 15 dBi) for MS, and 12 degrees (gain 24 dBi) for BS, respectively, the azimuth and elevation angles at BS and MS were varied in 12 and 30 degree steps, respectively.

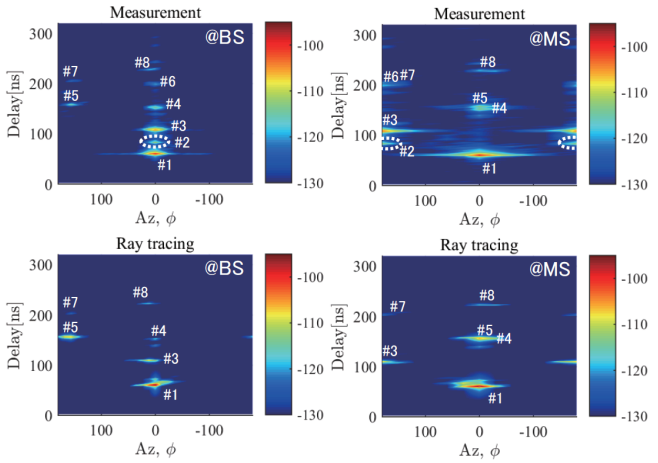

Fig. 2. Measured and simulated ADPSs seen from BS and MS.

3. Measurement Results

From the measured angle-resolved channel transfer functions for each polarization combination, the double-directional angle delay power spectrum (DDADPS) are obtained. The ADPS at both sides of the BS and MS as shown in Fig. 2 are synthesized from the DDADPS [5].

For precise interpretation of the measurement results, the RT simulation was used where the maximum orders of reflection and penetration were set to be three. The RT simulation employs the image method [7]. The first-order diffraction was further calculated based on uniform theory of diffraction (UTD). This simulation calculated the ray parameters of the received power, time delay of arrival, angles of departure (AoD) and arrival (AoA) for each path. For comparison with the measurement results, the simulation based DDADPS was reconstructed from the simulation results by applying the radiation patterns of the used antennas and the signal bandwidth of 400 MHz, then the RT-based ADPS were synthesized in the same manner as the measurement.

The ADPSs are shown in Fig. 2, where it can be seen that a few significant multi-path clusters are observed besides the penetrated path through the glass wall (GW) and the dominant paths in the RT results are well matched to those in the measurement results. In addition, comparing the measured and simulated ADPS of which power are overlapped on the panoramic environment photos and RT simulation results, the propagation mechanism of each cluster has been identified. The dominant clusters are presented in Table I showing delay, polarization combined path gain and relative polarimetric path gains for each cluster. From the results, it can be summarized as follows

- The dominant propagation mechanisms (20 dB less power than the free space LoS path) include multiple specular reflections on the indoor back wall (IBW) made by metallic door, GW and outdoor back wall (OBW) of the neighboring building with penetration into GW, thus the AoA and AoD are mainly aligned in LoS direction (0 degrees)

TABLE I
Identified Propagation Mechanisms

CL #	Mechanisms	Delay [ns]	Path Gain	$P_{\theta'\theta}$	$P_{\theta'\phi}$	$P_{\phi'\theta}$	$P_{\phi'\phi}$
1	P(GW)	0	-97.2	-2.19	-16.52	-17.94	1.26
2	Unidentified	22.5	-110.2	-0.42	-11.02	-8.19	-0.71
3	P(GW), R(IBW)	47.5	-102.7	-2.34	-14.02	-10.6	1.1
4	P(GW), R(IBW) R(GW)	92.5	-111.5	-2.37	(-11.85)	(-13.81)	1.17
5	R(OBW), P(GW)	97.5	-111.1	0.32	(-10.98)	(-13.02)	-1.11
6	P(GW), R(IBW), R(GW), R(IBW)	140	-116.1	-0.19	(-7.33)	(-9.63)	-1.32
7	R(OBW), P(GW) R(IBW)	145	-117.2	-0.24	(-6.67)	(-7.43)	-1.82
8	R(GW), R(OBW) R(GW)	167.5	-115	-0.02	(-8.55)	(-9.74)	-1.19

* P: Penetration, R: Reflection, GW: Glass Wall, IBW:Indoor Back Wall (metalic door), OBW:Outdoor Back Wall, and $y = (x)$ denotes $y \leq x$

- Eight significant multi-path clusters were observed, and those have relatively small power with the excess loss larger than 13 dB other than the first-order reflection from indoor back wall (CL#3).
- The measured transmission of P (GW) and reflection coefficients of R(BW) and R(GW) are approximately −4.5, −0.2 and −5.8 dB, respectively.
- The mechanism of CL#2 is not observed in RT simulation, but the integration occurs around the linear baffle ceiling. The excess loss of −13 dB is the second smallest and the cross-polarization ratio (XPR) of 7.5 dB is smallest.
- The scattering effect by some small objects was not significant except for CL#2.

Acknowledgment

This work was partly supported by JSPS KAKENHI Grant Number 15H04003.

References

[1] Maxwell, “Antennas and propagation for ISAP 2016,” IEICE The 5G Infrastructure Public Private Partnership (5G-PPP), https:// 5g-ppp.eu/

[2] “Channel Models for IEEE 802.11ay,”IEEE Document 802.11-15/1150r2, Sept. 2015.

[3] “Channel Models for 60 GHz WLAN Systems,” IEEE Document 802.11-09/0334r8, May 2010.

[4] Minseok Kim, Karma Wangchuk, Shigenobu Sasaki, Kazuhiko Fukawa, Jun-ichi Takada, “Development of Low Cost Mm-Wave Radio Channel Sounder and Phase Noise Calibration Scheme,” COST Action IC1004(EU), TD(15)12036, Jan. 2015 (Dublin, Ireland).

[5] M. Kim, K. Umeki, K. Wangchuk, J. Takada, S. Sasaki, “Polarimetric Mm-Wave Channel Measurement and Characterization in a Small Office,” Proc. PIMRC 2015, Aug. 2015.

[6] “Channel Model for Outdoor Open Area Access Scenarios,” IEEE Document 802.11-16/0342r1, Mar. 2016.

[7] Raplab, Kozo Keikaku Engineering Inc., http://www.kke.co.jp